Qiu et al. *Microsystems & Nanoengineering* (2025)11:203
https://doi.org/10.1038/s41378-025-00999-z

Microsystems & Nanoengineering
www.nature.com/micronano

ARTICLE Open Access

Microtube-integrated chips for modular electrical stimulation and 3D confined neural network growth

Ye Qiu[1,2], Xiaoduo Wang[1], Haibo Yu[1]✉, Jianchen Zheng[1,2], Jingang Wang[1,2], Lianqing Liu[1] and Wen Jung Li[1,3]✉

Abstract

In vitro neural networks offer a simplified model to study brain nervous system functions and represent a vital platform for investigating cerebral neural activities. Microelectrode array (MEA) chips are commonly used to construct modular neural networks and enable electrical stimulation and recording for uncovering signal generation and conduction mechanisms. However, conventional two-dimensional (2D) MEA chips face significant limitations, including restricted neuronal growth dimensions and insufficient neuron density. Herein, we present a novel micro-integrated chip featuring a three-dimensional (3D) physical microtube array that facilitates the regulated, confined growth of neurons. The microtube array not only provides a 3D microenvironment for neuronal growth and differentiation but also enhances neuronal network density and structural organization. Furthermore, by integrating the microtube array with a customized MEA, precise electrical stimulation can be applied to modular neural networks. Experimental results demonstrate that electrical stimulation effectively promotes the formation of connection pathways between adjacent 3D neural networks. Variable-parameter electrical stimulation experiments reveal that increasing voltage enhances the Young's modulus of neurons, highlighting the method's role in supporting the stable development of neuronal networks. This modular culture platform, combined with precise electrical stimulation, paves the way for constructing high-density 3D neuronal networks and enables synchronous control of modular neural activities. The proposed approach holds significant potential for advancing applications in neuroscience, tissue engineering, and organ-on-chip technologies.

Introduction

In recent years, neuronal cells culture in vitro used for the formation of neural networks has drawn escalating attention from researchers. Researches have indicated that the neural networks cultured in vitro exhibited similar neural activity characteristics to those observed in the brain[1–3]. This makes neural network culture in vitro a convenient option for studying neural activities, as it can be constructed using either cell lines or primary cells[4–6]. The induction and differentiation of neurons to form synapses can be accomplished through physical or chemical approaches[7,8]. Therefore, the advancement of in vitro culture techniques for neural networks is crucial for the construction of these networks and for fundamental neuroscience research.

MEA chips are widely used for stimulating and recording neuronal networks in vitro[9,10]. This technique relies on the direct contact of neuronal cells with microelectrodes and the formation of effective electrical connections, enabling precise signal recording at the single-neuron level[11,12]. Chunlian et al. utilized a 64-channel MEA chip to cultivate hypothalamic neural networks in an in vitro environment and conduct electrophysiological signal tests to achieve real-time blood glucose detection[13]. Shi et al. utilized a multi-step lithography method to fabricate a 128-channel PEDOT:PSS/PtNPs coated MEA

Correspondence: Haibo Yu (yuhaibo@sia.cn) or
Wen Jung Li (wenjli@cityu.edu.hk)
[1]State Key Laboratory of Robotics, Shenyang Institute of Automation, Chinese Academy of Sciences, Shenyang 110016, China
[2]University of Chinese Academy of Sciences, Beijing 100049, China
Full list of author information is available at the end of the article

© The Author(s) 2025
Open Access This article is licensed under a Creative Commons Attribution-NonCommercial-NoDerivatives 4.0 International License, which permits any non-commercial use, sharing, distribution and reproduction in any medium or format, as long as you give appropriate credit to the original author(s) and the source, provide a link to the Creative Commons licence, and indicate if you modified the licensed material. You do not have permission under this licence to share adapted material derived from this article or parts of it. The images or other third party material in this article are included in the article's Creative Commons licence, unless indicated otherwise in a credit line to the material. If material is not included in the article's Creative Commons licence and your intended use is not permitted by statutory regulation or exceeds the permitted use, you will need to obtain permission directly from the copyright holder. To view a copy of this licence, visit http://creativecommons.org/licenses/by-nc-nd/4.0/.

biosensor, significantly enhancing electrode performance for recording and electrical stimulation[14]. Evidently, the number of electrodes on the MEA chip is of paramount importance for the functionality of the neural network[15–17]. In 2020, Harvard University proposed a nanoelectrode array that successfully mapped excitatory and inhibitory synaptic connections from over 1,700 neurons[18]. More recently, Matteo et al. employed micro-nanofabrication processes to fabricate a 4096-channel multi-electrode array with asynchronous output compatible with neuromorphic processors[19]. As an invaluable tool for culturing and training neuronal networks in vitro, MEA chips have garnered considerable recognition in terms of universality and user-friendly nature. Nevertheless, it should also be noted that MEA chip technology confronts several challenges in applications. For instance, the distribution of neurons on microelectrodes is typically random, and continuous improvements are needed in reducing contact resistance and forming effective electrical connections[20,21].

To construct more controllable modular neural networks, researchers have employed physical and chemical methods to modify the surface of MEA chips[22,23]. Zhao et al. printed patterned peptide nanofibers on the substrate using inkjet printing, which guided the controllable directional distribution of neurons[24]. The Jordi team utilized a microcontact printing method based on PDMS stamps to coat the MEA chip with patterned poly-d-lysine, thereby constructing partitioned neural networks[25]. Zhe et al. established partitioned neural networks simulating the sensory and motor areas of the human brain by using patterned poly-d-lysine on the MEA chip[26]. Nevertheless, it has been indicated that chemical modification coatings have adverse effect on the electrode performance in MEAs, resulting in the deterioration of neural network functionality after a certain period of culture[27–29]. For this reason, researchers have proposed using physical microstructures to limit neuron growth for constructing modular neural networks[30]. The Gazzola group achieved partitioned neuron culture by adhering a porous PDMS film on the top of the MEA chip[31]. Shahrzad et al. combined PDMS microchannels with the MEA chip to cultivate modular neural networks with fixed connection modes[32]. Yoonkey's team used alginate hydrogel as a cell-repellent membrane and coated it on the surface of the MEA chip to cultivate orderly distributed neuron clusters[33]. The 2D planar partitioned neuron culture mode can expand the scale of neuron culture within certain limits and enabling investigation into signal transduction process between different neural networks[34]. However, 2D MEA chips still face limitations in scaling up neuron numbers and providing more suitable growth space for neurons[35,36].

In this paper, we proposed a facile new method for regulating the confined growth of neurons using physical microtube arrays. The greatest advantage of this method lies in the utilization of physical structures to induce the growth and differentiation of neurons, which can effectively maintain and enhance the activity of neuron cells. Furthermore, the microtube arrays possess a certain height that offers greater possibilities for the 3D growth of neurons and the increase of synaptic connection sites. By integrating with the patterned microelectrode array, the proposed chip structure can also provide modular electrical stimulation to neuron cells. Experimental results indicated that adjacent neuron networks are more prone to generating connection pathways when a direct current voltage of 5 mV is applied to the neural networks for 5 min per hour over 48 h. By contrast, neural networks without electrical stimulation only exhibited directional growth around the microtube arrays, and no connections formed between adjacent neuron networks. Through variable-parameter electrical stimulation experiments, it was further confirmed that the Young's modulus of neuron cells increases with the increase in voltage, indicating the beneficial effects of this method on neuron growth. Additionally, the modular cultivation mode demonstrates excellent potential in attaining higher neuron density and simulating the signal transmission behavior between neuron networks.

Results and discussion

Design and fabrication of microtube-microelectrode integrated chip

Figure 1a presents a schematic illustration of the principle for constructing the modular neural network. The integrated chip employed for building neural network modules in vitro primarily consist of coverslip, patterned microelectrode array, and microtube array. Notably, a layer of PDMS film is covered around the microtube array. The modular neural network discussed herein refers to the confined growth of neurons, restricting their growth to only the microtube arrays. This is attributed to the fact that the microtube array facilitates the growth and adhesion of neurons, thereby forming a spatial neural network. Simultaneously, the inhibitory effect of the PDMS film on neurons growth is also exploited. The patterned microelectrode array is utilized to mimic the functionality of the MEA chip, endowing it with a similar electrical stimulation capability for neurons as the MEA. Besides confining neurons growth within specific regions, the PDMS film also isolates the patterned microelectrode array from the culture medium solution, ensuring the formation of a uniform electric field by the microelectrode on the neural network. This modular neural network can not only simulate the interconnections behaviors between different neural network modules but also serve as a communication model among neural

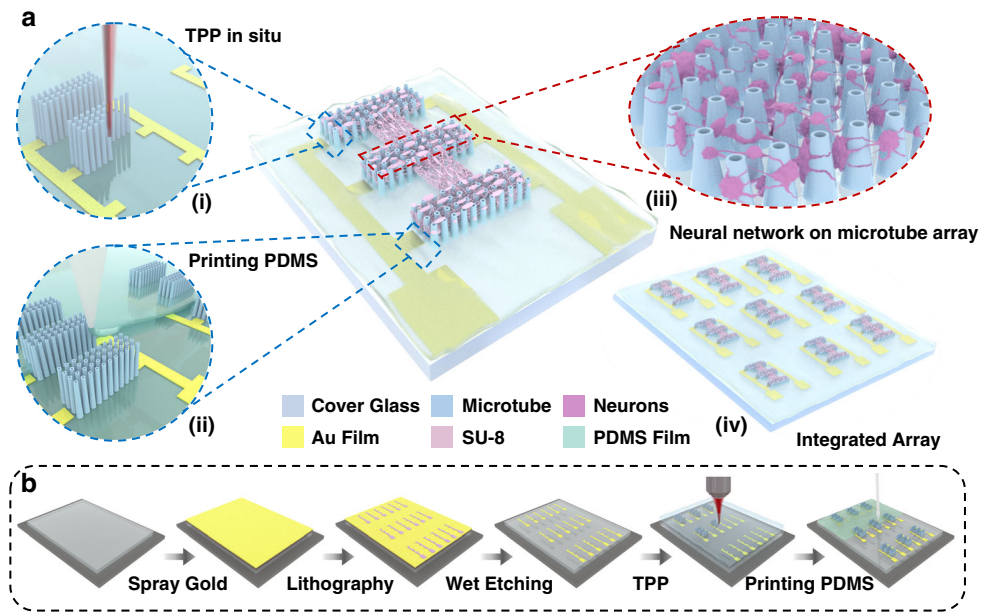


Fig. 1 The schematic diagram illustrating microtube-microelectrode integrated chip processing. a The schematic diagram showcases various stages of the microtube-microelectrode integrated chip, including in situ fabricating of a microtube array between electrodes using two-photon polymerization (i), coating a PDMS film around the microtube array (ii), the neural network grown on the microtube array (iii), and an array-based integrated chip formation (iv). **b** The processing process for the microtube-microelectrode integrated chip involves Au film deposition, maskless lithography, wet etching, two-photon polymerization, and E-jet printing

networks. Figure 1b showcases the various processing techniques utilized in the fabrication process of the modular neural network culture chip. Among them, photolithography and wet etching techniques are employed to fabricate the patterned microelectrode array on the coverslip. Two-photon polymerization (TPP) based on femtosecond laser is utilized for processing the on-demand customized microtube arrays. Furthermore, high-precision electrohydrodynamic jet printing (E-jet) technology is adopted to printing the PDMS films with controllable shapes. Given that fabricating processes involved in producing micro-integrated chip encompass diverse advanced micro-nano fabrication techniques, it becomes imperative to optimize each process meticulously in order to achieve high-quality integrated chip and thereby construct tailored modular neural networks.

Impact of morphological microstructures on neuron cultivation

As depicted in Fig. 2a, we accomplished the fabrication of diverse microstructures by altering the position of single-pulse exposure during the TPP process. Given that the thickness of the pre-cured photoresist film was 20 μm, the hollow microtube structures and solid micropillar structures could be obtained merely by modifying the focus spot position. The parameters of the microstructures are presented in Table 1. The inner diameter of the microtubes in Fig. 2b1 is 3 μm when the laser energy is fixed at 4.0 μJ, while it reduced to 1.5 μm in Fig. 2b2. Fig. 2b1 and 2b2 represent the SEM characterization of neurons growing on the microtube array, whereas Fig. 2b3 and 2b4 characterize the growth of neurons on the micropillar array. Through comparing these results, it was discovered that the number of neurons growing on the microtube array was significantly greater than that on the micropillar array after a culture period of 72 h. Neurons grown on microtube array can differentiate into more synaptic structures, and synaptic length increases significantly (Fig. S1). Further statistical analysis of the neuronal cell density on different microstructures revealed that the neuron density on the microtube array was markedly higher than that on the micropillar structure. The one-way ANOVA significance analysis further confirmed statistically significant differences ($p < 0.05$) in cellular density between microtube structure and micropillar structure. In statistical graphs, the letters a, b, and c denote statistically significant differences between data groups, while groups labeled with the same alphabetical character indicate the absence of significant differences ($p > 0.05$) as determined by post hoc statistical analysis. This finding aligns with morphological selectivity patterns observed in mechanosensitive cellular systems, reinforcing the critical role of topographical cues in regulating spatial cell distribution dynamics. Particularly when cultured for 72 h, the neuron density on the microtube array could reach 125.7 ± 1.2 cells/mL ($H_E = 30$ μm) and 107.5 ± 2.7 cells/mL ($H_E = 50$ μm), which was 1.5 times that on the micropillar

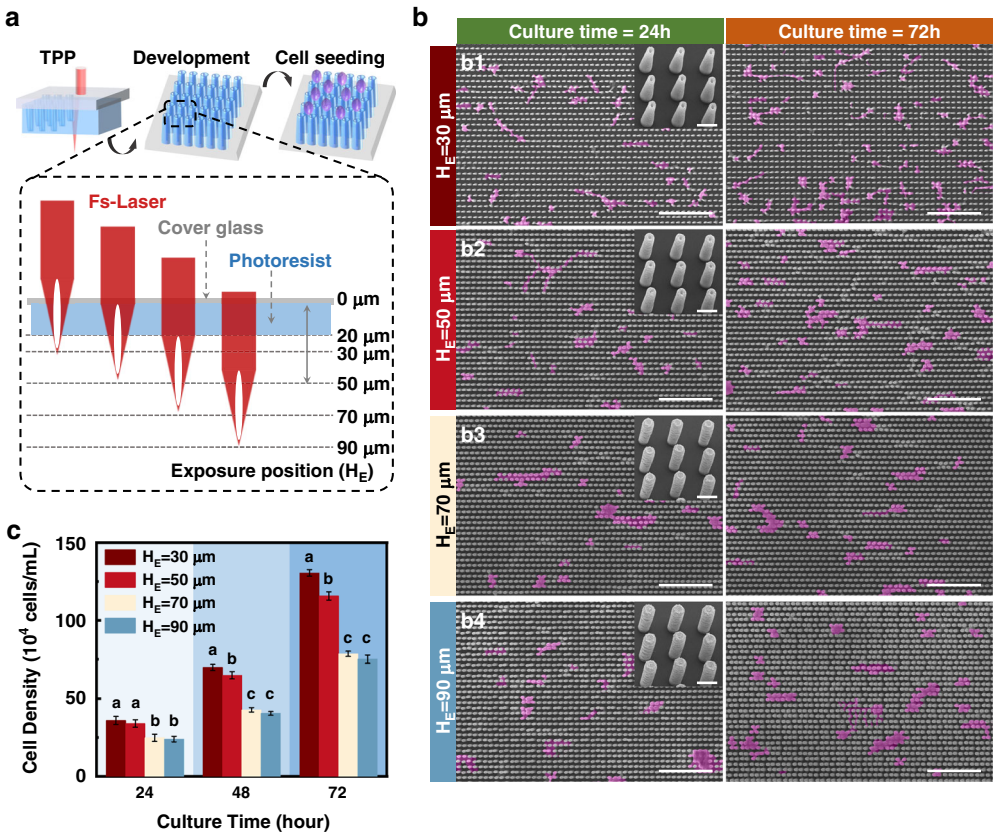


Fig. 2 The impact of microtube morphology on neuron growth. a Schematic diagram illustrating the implantation of neurons on the microtube array structure. The virtual frame displays the diagram of processing microtubes at varying processing heights. **b** Different morphologies of microstructures were utilized for in vitro neurons culture. The false color purple represents neurons. Scale bar: 100 μm. **b1**, **b2**, **b3**, and **b4** represent the microstructures at exposure positions of 30 μm, 50 μm, 70 μm, and 90 μm, respectively. The inset is the SEM representation of the microstructure. Scale bar: 10 μm. **c** Statistical plots depicting neuron density on microtube arrays with diverse morphologies. The sample size for each experiment is 200. The letters (**a**–**c**) on the bar chart were employed to denote statistically significant differences between groups ($p < 0.05$), while shared letters indicate no significant divergence

Table 1 Various parameters of different microstructures

Figure 2	Morphology	Inner diameter	Height	Exposure position	Pulse energy	Culture time
(b1)	Microtube	3 μm	20 μm	30 μm	4.0 μJ	24 h/48 h/72 h
(b2)	Microtube	1.5 μm	20 μm	50 μm	4.0 μJ	24 h/48 h/72 h
(b3)	Micropillar	0 μm	20 μm	70 μm	4.0 μJ	24 h/48 h/72 h
(b4)	Micropillar	0 μm	20 μm	90 μm	4.0 μJ	24 h/48 h/72 h

array (Fig. 2c). The above experimental finding indicates that the microtube structure is more favorable for the three-dimensional growth of neurons compared with the micropillar structure. The important reason for this is that the hollow structure of the microtube can accommodate more cell culture medium, providing more nutrients for the growth and development of neurons on its surface[37,38]. Moreover, microtube array can offer a 3D growth space for neurons promoting the construction of 3D neural network structures. Consequently, we selected the microtube structure array with $H_E = 30$ μm and an inner diameter of 3 μm for the 3D culture of neuron networks in subsequent experiments (Fig. S2).

3D Confined growth of neuron cells on microtube array

We constructed a 3D biological interface for the neuronal orientation and modular neural networks by integrating cell-friendly microtube arrays with cell-repellent

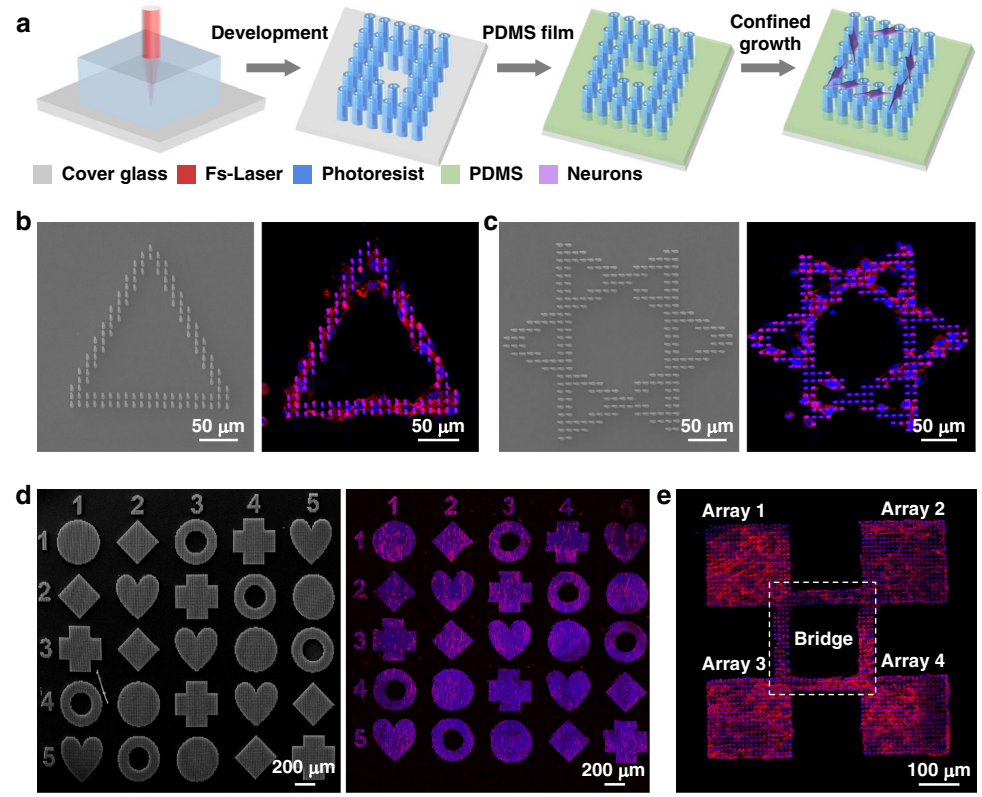


Fig. 3 Microtube structure array on neuronal confined growth. a Schematic diagram illustrating the confined growth of neurons. **b**, **c** Confined growth of neurons in the micrometer scale. Patterned triangular (**b**) and hexagonal (**c**) microtube structure, as well as fluorescence images depicting the confined neuronal growth. **d** Confined growth of neurons in the millimeter size. Large range microtube arrays with coordinate axes, each customized microtube array can be addressed independently. **e** Fluorescence diagram displaying interconnected neurons growing on the four microtube square array

PDMS films. Figure 3a presents the schematic illustration of the microstructure employed for the cultivation of modular neural networks. A PDMS film with a thickness of 2 μm was covered around the microtube array to confine the cell growth region, ensuring that the constructed neural network grows solely on the microtube array. The inhibitory effect of the PDMS film on the growth of neurons can be clearly observed from the comparative experiments in Supplementary Material S3. Then, we designed two types of patterned microtube arrays namely the triangular structure in Fig. 3b and the hexagonal structure in Fig. 3c for the directional induction of neurons. From fluorescence staining images of the cytoskeleton, it can be seen that the growth area of neurons precisely matches the shape of the microtube structure, and neurons are arranged orderly on the microtube structures. This implies that the microtube array fabricated by femtosecond laser-based two-photon polymerization not only possesses excellent biocompatibility but also is capable of guiding the directional distribution of neurons. Based on this, we extended this function of inducing the directional distribution of neurons to the millimeter-scale range for the confined growth of neurons. Figure 3d depicts a 5 × 5 square array composed of different patterned microtube arrays, with an area of ~2 mm × 2 mm. The fluorescence image indicates that neurons can all be restricted to the microtube structure arrays to achieve the confined growth of neural networks. In addition, each individual patterned array can be independently addressed using specific coordinates. For instance, [2, 3] represents the diamond-shaped microtube array located in the second row and third column. Furthermore, we established bridge structures with a width of 50 μm between different microtube arrays as shown in the Fig. 3e. It offers an approach for the structural interconnection and information interaction among modular neural networks, providing a more suitable model for studying the communication among modular neural networks.

Influence of electrical stimulation on the growth characteristics of neuron HT22

In contrast to the random interconnections of neurons forming neural networks, researchers prefer to induce the

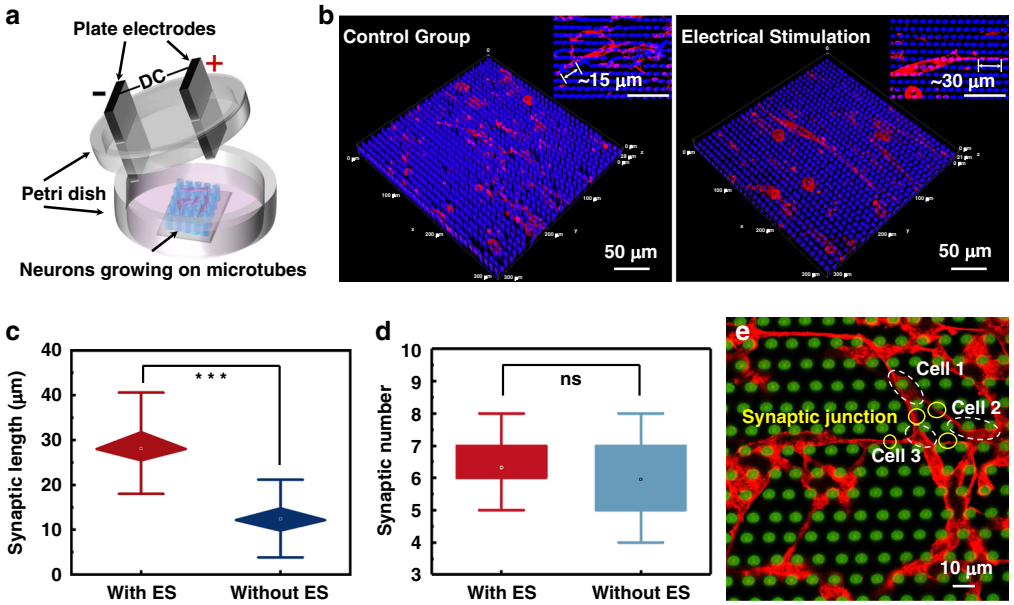


Fig. 4 The impact of electrical stimulation on neuronal activity. a The neurons cultured on the microtube array are subjected to electrical stimulation using a plate electrode. **b** The 3D fluorescence map depicting the morphology of neurons following electrical stimulation. The illustration represents a 2D fluorescence image captured from the top surface of the corresponding microtube structure. Scale bar: 50 μm. **c** Statistical maps displaying the length of synapses in electrically stimulated and non-stimulated neurons. **d** Statistical box plots illustrating the number of synapses of individual neurons with and without electrical stimulation. Student's *t*-test, ***($p < 0.001$), **($p < 0.01$), *($p < 0.05$), ns (non-significant). The sample size for each experiment is 200. **e** Fluorescent characterization of synaptic junctions after electrical stimulation. The dotted white lines indicate individual neurons, while the yellow circles represent synaptic connections

controllable neural networks to possess specific functions. According to the literature[39,40], electrical stimulation can enhance the microtube dynamics in the cytoskeleton, thereby promoting the growth and development of synapse structures and accelerating the interconnection of neurons to form neural networks[41]. Therefore, we used a pair of flat electrode to apply electrical stimulation to neuron HT22, with an electrode size of 15 mm × 20 mm and an inter-electrode spacing of 60 mm (Fig. 4a). The stimulation frequency was 5 min per hour and lasts for 72 h. It can be observed clearly from the fluorescence images that the synaptic length of the neurons significantly increased after electrical stimulation (Fig. 4b). Then, the synaptic length before and after electrical stimulation was statistically analyzed in the Fig. 4c. Prior to electrical stimulation, neurons exhibited a synaptic length of ~15 μm. However, this length increased up to 30 μm after electrical stimulation, which was twice that without electrical stimulation. This phenomenon indicates that electrical stimulation can promote the growth of synapse structures in hippocampal neuron HT22. According to the statistical results of the synaptic number within individual neurons (Fig. 4d), it can be found that there was no significant difference in the synaptic number on individual neurons before and after electrical stimulation, with a range of 5−7 (without ES) and 6-7 (with ES). Therefore, we conclude that electrical stimulation hardly facilitates an increase of the synaptic number in neuron HT22. The fluorescence staining image in Fig. 4e shows a single neuron differentiating into multiple synapse structures and establishing spatial physical connections with other neurons. This is also confirmed by the fluorescent image in the Fig. S4. Neuronal cells are connected by physical contact with synaptic structures that grow primarily from adherent microtube sidewalls. According to our previous research, the increase in HT22 neuron synaptic number mainly comes from the stimulation of 3D microtube structure morphology[42]. Therefore, we can effectively promote the growth of synaptic length and synaptic number simultaneously by combining the microtube array with electrical stimulation. This also is expected to provide effective technical support for the construction and communication of 3D modular neuronal networks in vitro.

Microelectrode array fabrication and electric field simulation

Precisely directed electrical stimulation is conducive to facilitating the functional realization of neural networks in vitro. In response to the deficiency of flexible precision electrical stimulation techniques for neural networks, we integrated the microtube array with the patterned microelectrode array and fabricated multiple micro-integrated chips applicable for precise electrical stimulation to 3D

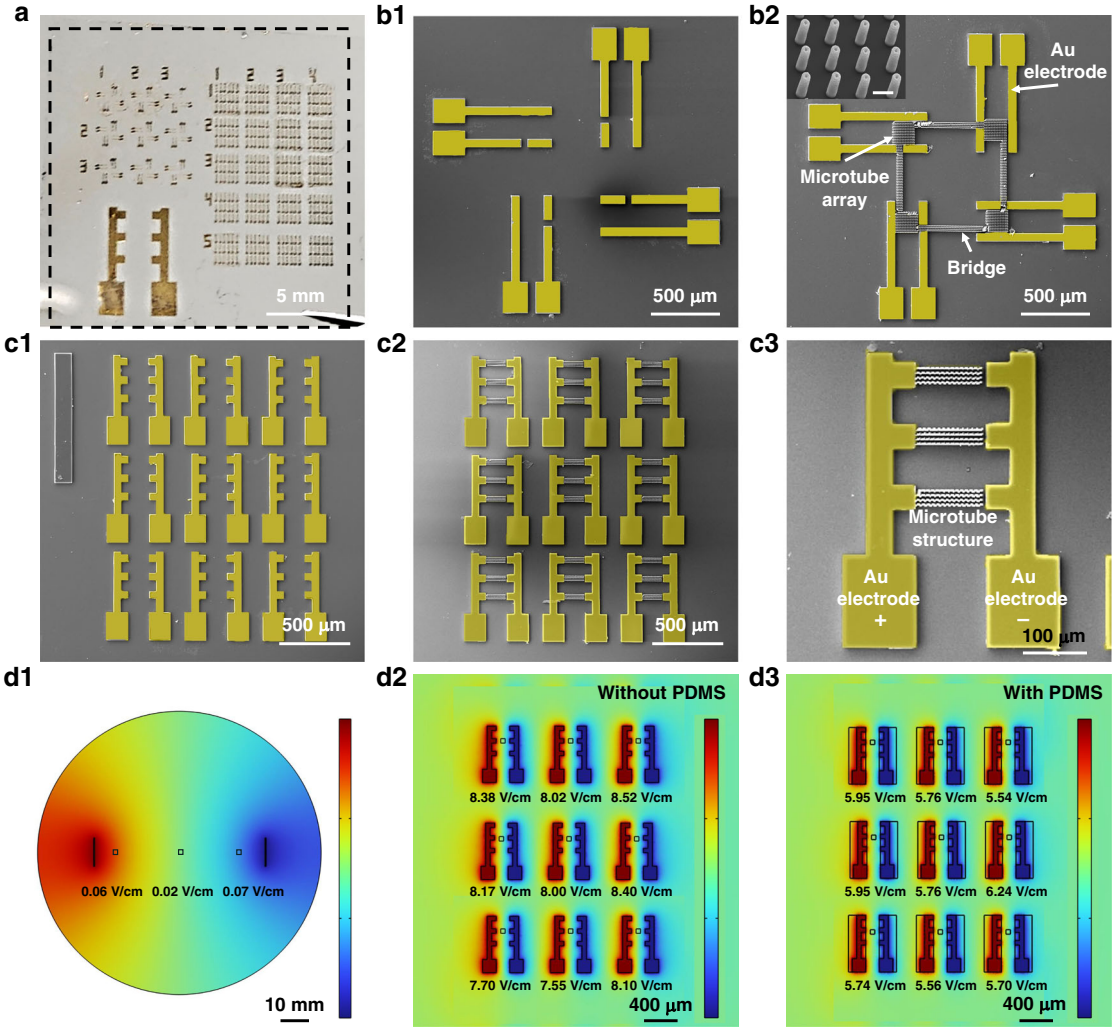


Fig. 5 Customized microelectrode arrays and electrical field simulation. a Physical depiction of various microelectrode arrays fabricated on a cover glass. The black dashed area is the cover glass. **b** SEM images showcasing four groups of microelectrodes. **b1** SEM images displaying four groups of strip microelectrodes. **b2** SEM characterization of four groups of strip microelectrodes with a microtube array, the inset exhibits an SEM magnification of the microtube structure, scale bar: 10 μm. **c** SEM characterization of the Interdigital-like microelectrode array. **c1** SEM characterization of the Interdigital-like microelectrode array. **c2** SEM characterization showing a microtube array after in situ machining on an Interdigital-like electrode, with (**c3**) providing a magnified view of a single Interdigital-like microelectrode in (**c2**). **d** Electric field simulation diagram illustrating different electrode structures. **d1** Electric field simulation of the flat electrode configuration. **d2** Electric field simulation depicting the design featuring an Interdigital-like microelectrode array. **d3** Electric field simulation showing the interdigital-like microelectrode array covered with a layer of PDMS film

modular neural networks. Figure 5a presents the different structural microelectrode arrays fabricated on a 22 mm × 22 mm coverslip using photolithography with wet etching, encompassing the strip microelectrode array (Fig. 5b1) on the left and the interdigital-like microelectrode array (Fig. 5c1) on the right. The microtube arrays can be fabricated in situ between each group of strip microelectrodes. Further, by using the microtube array as a bridge to connect the four groups of strip microelectrodes, we can obtain the interconnected micro-integrated chip depicted in Fig. 5b2. This structure can be employed to investigate the interconnection of different modular neural networks under the effect of electrical stimulation. Moreover, we can fabricate the parallel micro-integrated chip shown in Fig. 5c2 by fabricating microtube arrays in situ between the three pairs of fingertip structures of the interdigital-like microelectrodes. It is notable that to achieve the optimal electrical stimulation of the neural network on the microtube array, precise alignment between the microtube array and the fingertip structures are necessary (Fig. 5c3). Utilizing this structure, it is feasible to realize the partitioned cultivation of the neural network while concurrently conducting synchronous electrical stimulation on the neural networks in different regions.

To optimize the electrical stimulation parameters of the modular microelectrodes, we simulated the electric field distribution of the microelectrodes and made a comparison with that of the plat electrodes (Fig. 5d). A single microelectrode was set with a size of 100 μm × 400 μm × 50 nm, an inter-electrode spacing of 200 μm, and an applied voltage value of 150 mV. The simulation results indicated that the electric field distribution generated between the plat electrodes exhibited uneven distribution (Fig. 5d1). The electric field intensity decreased gradually from the edges of the electrode plates towards the center, with the electric field intensity at the center being merely 0.02 V/cm. In contrast, the electric field intensity at the center of the interdigital-like electrodes reached 8.19 ± 0.19 V/cm (Fig. 5d2), which was ~100 times that of the plat electrodes. Meanwhile, no electromagnetic interference was generated between adjacent interdigital-like electrodes. To investigate the influence of the PDMS film on the electric field distribution of the microelectrodes, we simulated the electric field distribution of the microelectrode array before and after printing the PDMS film. The results demonstrated that the electric field intensity of the microelectrodes covered with the PDMS film was 5.80 ± 0.22 V/cm (Fig. 5d3). It was at the same order of magnitude as that of the microelectrodes without the PDMS film, while the influence on the subsequent neuron electrical stimulation experiment could be negligible. The above findings suggest that compared with the conventional centimeter-scale plat electrode, the micro-integrated chip based on the modular microelectrode arrays can achieve higher efficiency and more precise electrical stimulation in the micrometer-scale regions of the neural network, better meeting the application requirements for precise and targeted neuron electrical stimulation.

Modular electrical stimulation of 3D neural networks with micro-integrated chip

In order investigate the regulatory role of modular micro-integrated chips in the growth characteristics of 3D neuron networks, we carried out experimental studies on the interconnection between neural network modules and synchronous variable-parameter electrical stimulation. We employed the interdigital-like parallel micro-integrated chip to perform electrical stimulation on different neural network modules using identical parameters, and observed the interconnections among adjacent neuron networks under electrical stimulation (Fig. 6a). The stimulation voltage was set at 5 mV, with 5 min of stimulation every hour. The neuron growth results after continuous culture for 72 h are presented in Fig. 6b. The adjacent neural network modules generated a connection with a width of ~25 μm after electrical stimulation, as indicated by the white dashed area in Fig. 6b. The neuronal cell HT22 forms the junctional pathway on the substrate composed of neuronal cells between two independent neuronal network modules through proliferation (Fig. S5). However, neurons without electrical stimulation only grow along the microtube array forming independent 3D neural networks. Based on the existing research progress[43,44], electrical stimulation can induce the ordered growth of synapses to form a well-developed neural network, and continuous electrical stimulation facilitates the establishment of interconnections between different neural network modules. Multiple repeated experiments have confirmed that independent neuronal network modules can stably establish connection pathways following targeted electrical stimulation (Fig. S6). Furthermore, it also confirmed the consistent functionality of micro-integrated chip in delivering precise electrical stimulation to neuronal networks, thereby validating its reliability as a neuromodulatory interface. Simultaneously, we investigated the mechanical properties of neurons under synchronous variable-voltage stimulation using the interconnected micro-integrated chip with four strip micoelectrodes (Fig. 6c). The stimulation voltages were set as 5 mV, 10 mV, 15 mV, and 20 mV respectively. Through the fluorescence images of the cytoskeleton (Fig. 6d), it can be observed that neurons exert a pulling force on the attached microtube structures under the influence of electrical stimulation, causing the microtube structure to tip towards the neuron. Moreover, an increase in tipped microtube structures was noted with higher levels of applied voltage. Young's modulus measurements were performed before and after electrical simulation revealing a significant increase in Young's modulus following electrical stimulation. And it increases progressively escalates with the increase of the stimulation voltage value. Significance analysis revealed statistically significant differences among the five experimental groups. These results confirm that the observed variations in cellular Young's modulus are primarily driven by voltage-induced alterations. When the stimulation voltage is 20 mV, the Young's modulus of neurons can reach 15 kPa, which is three times that of neurons without electrical stimulation (Fig. 6e). According to literature research, the increase of Young's modulus is mainly due to the fact that electrical stimulation promotes the formation of actin stress fibers and makes the cytoskeleton more dense. This helps cells resist external stress and maintain cell morphology in a dynamic environment, maintaining structural integrity and preventing lesions or loss of function caused by excessive morphology[45]. The experimental result indicated that the cytoskeleton of neurons can still maintain its integrity under voltage stimulation, facilitating the stable transmission of neuron signals and resisting changes in the external environment[46]. In addition to variable-voltage electrical stimulation, the micro-integrated chip with four strip micoelectrodes can also be used to administer variable-frequency electrical stimulation to four independent neuronal network

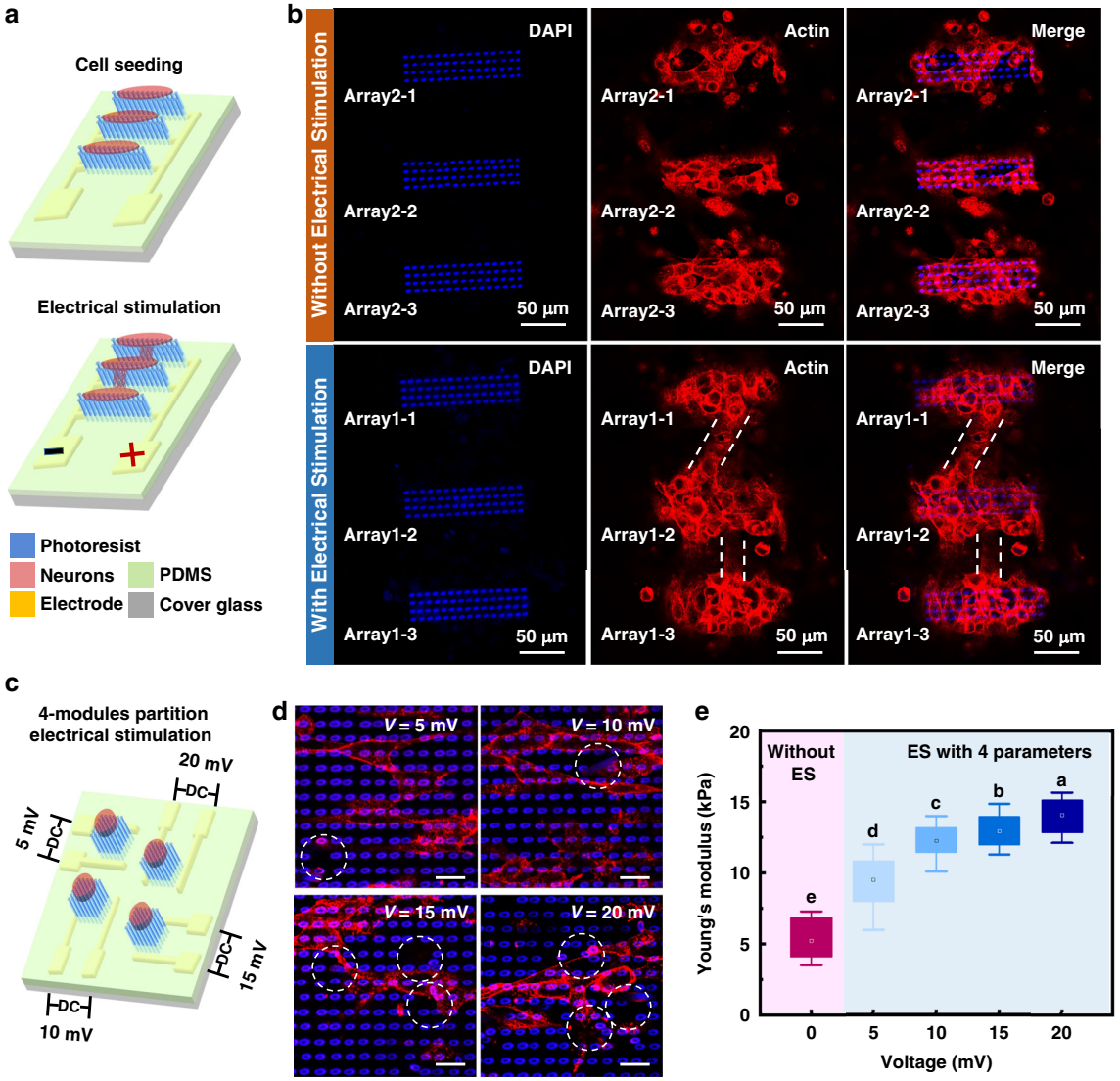


Fig. 6 The impact of modular electrical stimulation on neuronal activity. a Interdigital-like electrodes integrated unitized microtube arrays for electrical stimulation of neurons, comprising three microtube arrays functioning as a group for electrical stimulation. **b** Fluorescence image depicting the growth of neurons on three adjacent microtube arrays with/without electrical stimulation. **c** Schematic representation illustrating the integration of four pairs of electrodes and four sets of microtube arrays on a chip. **d** Fluorescence image of the neurons' morphology after applying simultaneous electrical stimulation on all four microtube arrays present on the same chip with voltage parameters of 5 mV, 10 mV, 15 mV, and 20 mV, respectively. **e** Statistical analysis of variations in Young's modulus of neurons under diverse electrical stimulation conditions. Scale bar: 20 μm. The sample size for each experiment is 200. The letters (**a**—**e**) on the bar chart were employed to denote statistically significant differences between groups ($p < 0.05$), while shared letters indicate no significant divergence

modules. Through the fluorescence map, it can be seen that under different frequencies of electrical stimulation, connecting pathways can be formed between neuronal networks (Fig. S7). We can also conclude that variable-frequency electrical stimulation has no significant effect on the construction of neural networks within 72 h. Both abovementioned structures are compatible with MEA chips and can achieve 3D confined growth of neurons, providing an excellent model for in vitro studies of modular 3D neuron networks.

The micro-integrated chip combined microtube structure and microelectrode arrays enables both confined growth of neuronal cells and precise electrical stimulation for modular 3D neuronal networks. Further research can enrich the functionality of the micro-integrated chip by integrating the electrophysiological signal recording function. Therefore, thereby establishing a closed-loop system capable of real-time neuronal activity monitoring and feedback-regulated stimulation. This technological advancement would ultimately achieve unified stimulation-detection operation for

primary neuronal cultures. Capitalizing on advancements in micro-nano fabrication technologies, strategic implementation of microfabricated metal recording sites on microtube sidewalls presents a viable pathway for three-dimensional neuronal signal acquisition. These 3D distributed recording elements enhance electrode integration density while enabling spatiotemporal signal characterization of neural networks. Furthermore, this technical framework may further extend to in vivo 3D signal detection applications. The convergence of 3D neural signal recording architectures with electrical stimulation modalities is expected to become the core technology of next-generation neural interfaces and promote their application breakthroughs in neuroscience research and clinical treatment.

Conclusion

In this work, we developed a modular micro-integrated chip that combines microelectrodes with microtube arrays, fabricated through advanced micro-nano processing techniques, including a TPP process. This platform successfully enabled the construction of modular 3D neural networks in vitro, providing precise and controllable micrometer-scale electrical stimulation. Compared to conventional micropillar structures, the microtube arrays demonstrated superior performance in supporting 3D neuronal culture, offering enhanced spatial confinement and promoting neuron differentiation. Additionally, by precisely coating PDMS films around the microtube arrays, we created a multifunctional 3D biological interface with differential cell affinity properties, facilitating the cross-scale confined growth of neurons into organized modular networks. The integration of patterned microelectrodes further enabled the application of localized and uniform electric fields, as confirmed by simulation analyses, which demonstrated higher-intensity and more homogeneous stimulation compared to planar electrodes. Experimental results showed that electrical stimulation effectively promoted the formation of interconnection pathways between adjacent modular neural networks. Furthermore, the interconnected micro-integrated chip, equipped with four sets of strip microelectrodes, allowed simultaneous application of variable-voltage stimulation to multiple neural network modules. Mechanical characterization revealed that higher stimulation voltages significantly increased the Young's modulus of neurons, highlighting the potential to modulate neuronal properties and control inter-module communication. This innovative platform provides a flexible and precise tool for studying 3D modular neural networks, bridging the gap between in vitro and in vivo systems. It holds significant promise as a complementary platform for advancing neuroscience research, as well as applications in tissue engineering and organ-on-chip technologies.

Materials and methods

Fabrication of patterned microelectrode array

To realize the high-precision layout and high conductivity of the patterned microelectrode array, we fabricated the Au microelectrode array structure by combining photolithography and wet etching. Firstly, a high-conductive metal Au layer including a Cr thin layer (5 nm) and an Au layer (50 nm) was deposited on the cover glass using a magnetron sputtering system (PECVD400, Sky Technology Development, China), where the Cr layer acted as an adhesion layer between the Au layer and the cover glass. Subsequently, we selected negative photoresist SU-8 (2015, Cchip Scientific Instrument, China) as the mask and selectively cured the photoresist using maskless photolithography (DaIi, Aresis, Slovenija) following the patterned microelectrode structure. After photolithography and development, the cured photoresist in the shape of the microelectrode pattern remained on the surface of the Au layer serving as the mask for wet etching. The fabricated samples were separately immersed in the Au etching solution (for 30 s) and the Cr etching solution (for 30 s) to remove the excess metals Au and Cr. The Au etching solution was prepared by mixing iodine, potassium iodide, and deionized water in a mass ratio of 1:4:20. The Cr etching solution was prepared by dissolving ammonium cerium nitrate (4 g) and glacial acetic acid (1 mL) in 20 g of deionized water. After etching off the excess metals, the metal electrodes with the photoresist mask remained. Subsequently, the samples were immersed in the SU-8 gel removal agent (SU-8, Cchip Scientific Instrument, China) for 11 min to remove the excess photoresist leaving only the clean microelectrode array.

Fabrication of microtube-microelectrode integrated chips

The fabricated Au microelectrode arrays were spin-coated with a 20 μm thick layer of photoresist (SZ2080, Forth, Greece) and pre-cured at 100°C for 1 h. Then, we placed the sample on a micromaching system based on the femtosecond laser (Pharos-6 W, Light conversion, Lithuania) to fabricate the microtube arrays in situ. Firstly, we modulated the initial Gaussian light spot shape to an annular light spot utilizing a dual-aperture optical modulation method to create to a cavity structure along the laser propagation direction. Thus, by precisely aligning the cavity structure with the photoresist to obtain the microtube structures with a high aspect ratio, as described in our previous work[42]. Meanwhile the combination of the micro piezo motion platform with the macro large-scale motion platform ensured large-scale high-precision processing. Additionally, a CCD imaging system was utilized for real-time imaging monitoring of the processing process. The fabrication of the microtube structure is primarily based on the femtosecond laser single-pulse two-photon polymerization. The developer solution was

prepared by mixing n-propanol and isopropanol in a volume ratio of 1:1, and the development time was set at 14 min. Finally, the sample was soaked in isopropanol for 10 min to remove the unpolymerized photoresist.

Construction of cell-repellent interface

The cell-repellent interface is primarily constructed with PDMS films. Firstly, the PDMS prepolymer (184, DOWSIL, US) and curing agent (184, DOWSIL, US) are uniformly mixed at a mass ratio of 10:1, and air bubbles are removed using a heating vacuum machine (DZF-6012, yiheng, China). Subsequently, we employed a self-assembled E-jet printing system to printing the PDMS prepolymer. The diameter of the printing needle tube is set at 20 μm, the driving voltage is 800 V, and the printing speed is 0.01 mm/s. The area surrounding the microtube arrays is coated with a 2 μm-thick PDMS layer by controlling the motion path of the motion platform. Finally, the PDMS is heated at 100°C for 30 min to cure it into a film.

Characterization

To precisely observe the layout of the microtube structure and the microelectrode structure, we characterized the microelectrode arrays and microtube structures by using a scanning electron microscope (Quattro S, Thermostatic, US). Besides, the detailed distribution of neurons on the microtube array was also characterized through the SEM. The Young's modulus of the cells was measured using a self-built atomic force microscopy system in which a cantilever micropipette probe (1B 100 F-4, Sutter Instrument, Inc., America) was used as a scanning probe to accurately measure the Young's modulus of the cells[47].

Cell culture

The cells employed in this study are hippocampal neurons HT22 of rats, which is purchased from Jiangsu Keygen Biotechnology Co., Ltd. Cell culture medium-high glucose (DMEM, Gbico, USA) was supplemented with 10% fetal bovine serum and 1% penicillin/streptomycin. Neurons were cultured at 37°C with a CO_2 concentration of 5%. For the sterilization of the samples, the fabricated samples were soaked in 75% alcohol for 30 min and then irradiated under ultraviolet light for 1 h. Subsequently, the samples were rinsed three times with PBS buffer (DT20012, Deary, China) to complete the pretreatment of the samples. Neurons were first rinsed twice with PBS buffer to remove impurities and dead cells. Next, the cells were digested with trypsin for 30 s, and then adding cell culture medium to stop the digestion process. The adherent-growing cells were blown and sucked with a pipette to form a cell suspension. The cell density of neurons was calculated using a cell counting plate, the seeding density of neurons in this experiment was 20×10^4 cell/mL.

Experimental configuration of electrical stimulation

The electrical stimulation system for neurons is mainly composed of electrodes, wires and a multi-channel electrical stimulator (Master-9, AMPI, Israel). The parameters such as the type, frequency and period of the output signal are controlled by computer software. Here, we employ direct current voltage as the electrical stimulus signal, with a stimulation frequency of 5 min per hour and a stimulation period of 72 h. The size of a single microelectrode is ~100 μm × 400 μm × 50 nm, and the spacing between electrodes is 200 μm, which is connected to the multi-channel electrostimulator through pins. The size of the plat platinum (Pt) electrode is 15 mm × 20 mm × 0.1 mm. The plat electrodes are vertically embedded in the lid of the culture dish, and the spacing between the electrodes is 60 mm. The lid of the culture dish is placed on the culture dish to ensure that the lower end of the plat electrode can contact the bottom of the culture dish, so as to provide a relatively uniform electric field for the neurons therein.

Fluorescent characterization of cells

We opted to stain the cell nuclei and actin to further visualize the morphology and distribution of neurons. Firstly, using 4% paraformaldehyde (Cat # P1110, Solarbio, China) to fix the cell morphology and position. The sample was immersed for 20 min and then washed three times with PBS to remove the residual reagents. Subsequently, 5 μL of Actin Tracker Red-555 solution (C2203S, Beyotime, China) was diluted in 1 mL of PBS. The diluted solution was used to submerge the sample and incubated at room temperature in the dark for 60 min. Then the sample was washed with PBS three times again. Finally, DAPI (C1005, Beyotime, China) was used to stain the neuronal nuclei. The sample was immersed in the DAPI solution and incubated at room temperature in the dark for 15 min. The sample was washed with PBS three times again to remove the excess reagents. Finally, a confocal laser microscope (A1, Nikon, Japan) was used to capture the fluorescent images of the morphology and distribution of neurons.

Acknowledgements

This work was supported by the National Key R&D Program of China (Project No. 2022YFB4700100), the Innovation Promotion Research Association of the Chinese Academy of Sciences (NO. 2022199), the Applied Basic Research Program of Liaoning Province (NO. 2023JH2/101600037), the National Natural Science Foundation of China (Grant No. 62403454 and 62303446), and the Hong Kong Research Grants Council (NO. 11216120).

Author details

[1]State Key Laboratory of Robotics, Shenyang Institute of Automation, Chinese Academy of Sciences, Shenyang 110016, China. [2]University of Chinese Academy of Sciences, Beijing 100049, China. [3]Department of Mechanical Engineering, City University of Hong Kong, Hong Kong 999077, China

Conflict of interest

The authors declare no competing interests.

Supplementary information The online version contains supplementary material available at https://doi.org/10.1038/s41378-025-00999-z.

Received: 18 December 2024 Revised: 2 May 2025 Accepted: 29 May 2025
Published online: 31 October 2025

References

1. Tan, H. Y., Cho, H. & Lee, L. P. Human mini-brain models. *Nat. Biomed. Eng.* **5**, 11–25 (2021).
2. Hong, N. & Nam, Y. Neurons-on-a-chip: in vitro neurotools. *Mol. Cells* **45**, 76–83 (2022).
3. Wang, Y., Liu, S., Wang, H., Zhao, Y. & Zhang, X. D. Neuron devices: emerging prospects in neural interfaces and recognition. *Microsyst. Nanoeng.* **8**, 128 (2022).
4. Andolfi, A., Jang, H., Martinoia, S. & Nam, Y. Thermoplasmonic Scaffold design for the modulation of neural activity in three-dimensional neuronal cultures. *BioChip J.* **16**, 451–462 (2022).
5. Han, X. et al. A functional neuron maturation device provides convenient application on microelectrode array for neural network measurement. *Biomater. Res.* **26**, 84 (2022).
6. Liu, Y. et al. Nanomaterial-based microelectrode arrays for in vitro bidirectional brain-computer interfaces: a review. *Microsyst. Nanoeng.* **9**, 13 (2023).
7. Beck, C. L., Killeen, C. T., Johnson, S. C. & Kunze, A. Nanomagnetic guidance shapes the structure-function relationship of developing cortical networks. *Nano Lett.* **24**, 13564–13573 (2024).
8. Duru, J. et al. Engineered biological neural networks on high density cmos microelectrode arrays. *Front. Neurosci.* **16**, 829884 (2022).
9. Vallejo-Mancero, B., Faci-Lazaro, S., Zapata, M., Soriano, J. & Madrenas, J. Real-time hardware emulation of neural cultures: a comparative study of in vitro, in silico and in duris silico models. *Neural Netw.* **179**, 106593 (2024).
10. Leng, Y. et al. Advances in in vitro models of neuromuscular junction: focusing on organ-on-a-chip, organoids, and biohybrid robotics. *Adv. Mater.* **35**, e2211059 (2023).
11. Zhang, H. et al. Single neurons on microelectrode array chip: manipulation and analyses. *Front. Bioeng. Biotechnol.* **11**, 1258626 (2023).
12. Kasuba, K. C. et al. Mechanical stimulation and electrophysiological monitoring at subcellular resolution reveals differential mechanosensation of neurons within networks. *Nat. Nanotechnol.* **19**, 825–833 (2024).
13. Qin, C. et al. Biohybrid tongue based on hypothalamic neuronal network-on-a-chip for real-time blood glucose sensing and assessment. *Biosens. Bioelectron.* **244**, 115784 (2024).
14. Xu, S. et al. High-throughput PEDOT:PSS/PtNPs-modified microelectrode array for simultaneous recording and stimulation of hippocampal neuronal networks in gradual learning process. *ACS Appl. Mater. Interfaces* **14**, 15736–15746 (2022).
15. Brofiga, M. et al. Multiple neuron clusters on micro-electrode arrays as an in vitro model of brain network. *Sci. Rep.* **13**, 15604 (2023).
16. Geng, L. et al. A 1280-Channel neural microelectrode array with complementary wedge-shaped 3-D assembly interfaces. *IEEE Sens. J.* **24**, 13841–13855 (2024).
17. Duru, J. et al. Investigation of the input-output relationship of engineered neural networks using high-density microelectrode arrays. *Biosens. Bioelectron.* **239**, 115591 (2023).
18. Abbott, J. et al. A nanoelectrode array for obtaining intracellular recordings from thousands of connected neurons. *Nat. Biomed. Eng.* **4**, 232–241 (2020).
19. Cartiglia, M. et al. A 4096 channel event-based multielectrode array with asynchronous outputs compatible with neuromorphic processors. *Nat. Commun.* **15**, 7163 (2024).
20. Tibau, E., Ludl, A.-A., Rudiger, S., Orlandi, J. G. & Soriano, J. Neuronal spatial arrangement shapes effective connectivity traits of in vitro cortical networks. *IEEE Trans. Netw. Sci. Eng.* **7**, 435–448 (2020).
21. Prox, J., Smith, T., Holl, C., Chehade, N. & Guo, L. Integrated biocircuits: engineering functional multicellular circuits and devices. *J. Neural Eng.* **15**, 023001 (2018).
22. Yamamoto, H. et al. Modular architecture facilitates noise-driven control ofsynchrony in neuronal networks. *Sci. Adv.* **9**, eade1755 (2023).
23. Sato, Y. et al. Microfluidic cell engineering on high-density microelectrode arrays for assessing structure-function relationships in living neuronal networks. *Front. Neurosci.* **16**, 943310 (2022).
24. Sun, W. et al. Cell guidance on peptide micropatterned silk fibroin scaffolds. *J. Colloid Interface Sci.* **603**, 380–390 (2021).
25. Yamamoto, H. et al. Impact of modular organization on dynamical richnessin cortical networks. *Sci. Adv.* **4**, eaau4914 (2018).
26. Chen, Z. et al. A modular biological neural network-based neuro-robotic system via local chemical stimulation and calcium imaging. *IEEE Robot. Autom. Lett.* **8**, 5839–5846 (2023).
27. Park, M. U. et al. Collective dynamics of neuronal activities in various modular networks. *Lab Chip* **21**, 951–961 (2021).
28. Yoon, D. & Nam, Y. A 3D neuronal network read-out interface with high recording performance using a neuronal cluster patterning on a microelectrode array. *Biosens. Bioelectron.* **261**, 116507 (2024).
29. Gladkov, A. et al. Design of cultured neuron networks in vitro with predefined connectivity using asymmetric microfluidic channels. *Sci. Rep.* **7**, 15625 (2017).
30. Forro, C. et al. Modular microstructure design to build neuronal networks of defined functional connectivity. *Biosens. Bioelectron.* **122**, 75–87 (2018).
31. Zhang, X. et al. Mind in vitro platforms: versatile, scalable, robust, and open solutions to interfacing with living neurons. *Adv. Sci.* **11**, e2306826 (2024).
32. Habibey, R. et al. Engineered modular neuronal networks-on-chip represent structure-function relationship. *Biosens. Bioelectron.* **261**, 116518 (2024).
33. Lee, H., Yi, G. S. & Nam, Y. Connectivity and network burst properties of in-vitro neuronal networks induced by a clustered structure with alginate hydrogel patterning. *Biomed. Eng. Lett.* **13**, 659–670 (2023).
34. Suzuki, I. et al. Large-area field potential imaging having single neuron resolution using 236 880 electrodes CMOS-MEA technology. *Adv. Sci.* **10**, e2207732 (2023).
35. Peng, H. et al. Laser-patterned epoxy-based 3D microelectrode arrays for extracellular recording. *Nanoscale* **16**, 14295–14301 (2024).
36. Vajrala, V. S., Elkhoury, K., Pautot, S., Bergaud, C. & Maziz, A. Hollow ring-like flexible electrode architecture enabling subcellular multi-directional neural interfacing. *Biosens. Bioelectron.* **227**, 115182 (2023).
37. Fan, S. et al. Accelerating neurite growth and directing neuronal connections constrained by 3d porous microtubes. *Nano Lett.* **22**, 8991–8999 (2022).
38. Youngblood, R. L., Sampson, J. P., Lebioda, K. R. & Shea, L. D. Microporous scaffolds support assembly and differentiation of pancreatic progenitors into beta-cell clusters. *Acta Biomater.* **96**, 111–122 (2019).
39. Yang, H. et al. Gold nanostrip array-mediated wireless electrical stimulation for accelerating functional neuronal differentiation. *Adv. Sci.* **9**, e2202376 (2022).
40. Brown, M. A. et al. Direct laser writing of 3D electrodes on flexible substrates. *Nat. Commun.* **14**, 3610 (2023).
41. Poli, D. & Massobrio, P. High-frequency electrical stimulation promotes reshaping of the functional connections and synaptic plasticity in in vitro cortical networks. *Phys. Biol.* **15**, 06LT01 (2018).
42. Qiu, Y. et al. Engineering 3D microenvironments with femtosecond laser-fabricated microtubes to direct neuronal network formation. *Addit. Manuf.* **88**, 104249 (2024).
43. Meng, X. et al. Electrical stimulation induced structural 3D human engineered neural tissue with well-developed neuronal network and functional connectivity. *J. Neural Eng.* **20**, 20 (2023).
44. Tai, Y. et al. Formation of 3D self-organized neuron-glial interface derived from neural stem cells via mechano-electrical stimulation. *Adv. Health. Mater.* **10**, e2100806 (2021).
45. Wang, T. et al. Rehabilitation exercise-driven symbiotic electrical stimulation system accelerating bone regeneration. *Sci. Adv.* **10**, eadi6799 (2024).
46. Yang, H. et al. A microfluidic platform integrating dynamic cell culture and dielectrophoretic manipulation for in situ assessment of endothelial cell mechanics. *Lab Chip* **23**, 3581–3592 (2023).
47. Shi, H. et al. Automated force curve methods based micropipette force sensors. In *IEEE Transactions on Nanotechnol*, 224—230 (IEEE, 2024).